Materials Research. 2024; 27:e20230496
DOI: https://doi.org/10.1590/1980-5373-MR-2023-0496

Reduction Kinectics of Hematite Powders in Non-Equilibrium Hydrogen Plasma

Iraldo Sá Silveira[a], Estéfano Aparecido Vieira[a], Ramiro Conceição Nascimento[a], Adonias Ribeiro Franco Júnior[a], Jaime Alberto Sanchez Caceres[a]*

[a]Instituto Federal do Espírito Santo, Departamento de Engenharia Metalúrgica e de Materiais, Vitória, ES, Brasil.

Received: November 13, 2023; Revised: March 18, 2024; Accepted: May 02, 2024

The reduction kinetics of hematite (Fe_2O_3) powders was studied using nonequilibrium hydrogen plasma as reducing agent. Reduction experiments were performed in a *DC* pulsed plasma reactor, hydrogen flow-rate of 300 cm^3/min, at pressure of 400 Pa, reduction times in range 30-120 minutes and in temperatures range 320-380 °C. Fe_2O_3 powders after reduction experiments were characterized by X-ray diffraction, weight loss of oxygen (gravimetric analyses), optic microscope and scanning electron microscope. The results showing that the reduction temperature of 380 °C after 120 min allows obtaining α-iron with a reduction fraction of about 0.93. The powder particles are transformed into two steps: $Fe_2O_3 \rightarrow Fe_3O_4 \rightarrow$Fe-α. The activation energy experimentally established for the reduction of Fe_2O_3 was about 98.4 kJ/mol.

Keywords: *Hematite reduction, Hydrogen plasma, Solid-state reaction, Activation energy.*

1. Introduction

The carbothermic reduction methods have been used since antiquity for extracting metals from their ores[1]. New reduction routes have been proposed from 1970's by several research groups, attempting to mitigate the generation of both solid wastes and greenhouse effect gases. Among the proposals, one can mention: metal oxide direct reduction using hydrogen gas as reducing agent, vacuum carbothermic reduction, direct electrochemical reduction of solid refractory oxide in molten magnesium chloride (Cambridge Process), metallothermic reduction, and high-energy milling[2-7].

The development of process based on the use of hydrogen as reducing agent constitutes very interesting alternative, given the possibility of direct use of fine ore avoiding previous treatments such as sintering and pelletizing. It is possible the elimination of greenhouse gas emissions and generation of only water steam. However, the deployment and industrial rise of hydrogen reduction methods based on the high cost of production due to hydrocarbon reform steps or hydrolysis of water[8].

The potential for application of cold plasma, also known as non-equilibrium plasma, in metal reduction has been demonstrated experimentally by different research groups over the last 10 years[9-15]. In 2003, Silva[9] shows that between 600 °C and 800 °C the kinetics of reduction of tungsten oxide (WO_3) by cold plasma of hydrogen is much bigger than the hydrogen gas. The following year Zhang et al.[10] published a work showing that at the temperature of 200 °C copper oxide (CuO) is totally reduced to metallic copper (Cu) after 2 h of experiment, that did not occur when hydrogen gas was used. Recently, Rajput et al.[12] showed that from the Hematite (Fe_2O_3) may be obtained with metallic iron reduced fractions (α) of 0.94 after 2 h at 300 °C temperature in microwave plasma reactor of 2.45 MHz. According to information contained in this work, the kinetics of reduction of Hematite by hydrogen gas (H_2) is comparable to the reduction by hydrogen plasma only from temperatures above 800 °C. Nakayama[13] shows that the cold plasma of hydrogen as reducing agent provides a considerable increase in reduction kinetics of powders of cobalt oxide (Co_3O_4), for reducing temperatures between 250 °C and 300 °C. At 250 °C, the plasma allowed get fractional reduction around 0.90 after 50 min of reduction. In these same conditions, the use of gas resulted in fractions of the maximum reduction of just 0.30.

The Ellingham diagram-Richardson[16] shows that the atomic hydrogen (H), one among the many species present in plasma, is capable of reducing the various existing oxides in low temperatures. The collision of these electrons, energy-dense, with gas molecules can result in excitation, ionization, dissociation, production of electrons and, among other reactive species, in the formation of atomic hydrogen[11,17]. Dissociation reactions increase the kinetics of reduction since the same foster production of atomic hydrogen (H), species able to diffuse through the oxide structure[18,19].

2. Materials and Methods

This work used samples of Hematite powder with a granulometry in the range from 1 μm to 5 μm which corresponded the mass 80% used with purity was above 99.0%. To promote the reduction was used hydrogen gas by the company White Martins®. The purity of the gas is 99.999% according to the supplier.

*e-mail: jcaceres.vix@gmail.com

2.1. Plasma-assisted reduction experiments

A DC pulsed plasma reactor (Thor NP design, supplied by SDS Plasma Company®, Paranrá, Brazil) was used to carry out the reduction tests, Figure 1.

The reactor consists of a Board of 50 cm diameter by 75 cm high voltage pulsed voltage source 650 V maximum and 3.4 kHz frequency, mechanical pump with ability to achieve pressures below 1.0 Pa, with maximum flow meter H_2 of 500 cm^3/min, thermocouples for temperature monitoring of samples and external heating system for heating of samples until the working temperature before the activation of the plasma. The heating was accomplished through an electrical resistance accoupled at the cathode.

The experimental conditions of the hematite reduction process by cold hydrogen plasma were employed the following parameters: voltage between electrodes of 540 V, 400 Pa pressure, and hydrogen flow of 300 cm^3/min. The experiments were conducted in temperatures range 320-380 °C, and reductions times range in 30-120 minutes. Each experiment was used five samples contained in 316 L stainless steel crucibles, totaling eighty samples. The initial mass of each one of the samples was approximately 200 mg of hematite.

2.2. Gravimetry

After the hematite reduction process, the plasma was interrupted and the samples cooled still inside the reactor chamber under vacuum to room temperature. The mass of powders, before and after the reduction experiments, was determined by gravimetric method, using a scale from OHAUS Explorer precision model brand of 0.1 mg. The reduced fraction determination, α, was done as follows (Equation 1):

$$\alpha = \frac{M_H}{3.M_O}.\left(\frac{m_i - m_f}{m_i}\right) \approx 3{,}33.\left(\frac{m_i - m_f}{m_i}\right) \quad (1)$$

where: α is fraction of reduction, (mi) is the initial mass, (mf) is the final mass, M_H is the molecular weight of hematite worth approximately 160 g and M_O is the molecular weight of oxygen worth 16 g.

From the data of α, it was possible to trace the curves fraction of reduction (α) x time and reduction determine the activation energy (Ea) for the hematite reduction process particles by hydrogen plasma.

2.3. X-ray diffraction

The reduction products obtained in different experimental conditions were qualitatively identified through analysis by X-Ray diffraction (XRD). We used a model D2 diffractometer Phaser brand Bruker with $K_{\alpha\text{-}Cu}$ radiation with a wavelength of 1.54 Å. Powders samples were employed with mass between 700 and 1.000 mg. The parameters for measurements were as follows: time of 0.3 s, count with 2θ ranging from 10° to 80°, step of 0.02° in 2θ and 5 rotation speed rpm.

2.4. Microstructural analysis

After the experiments, the powders reduced samples were analyzed by o light microscope and scan electronic microscopy.

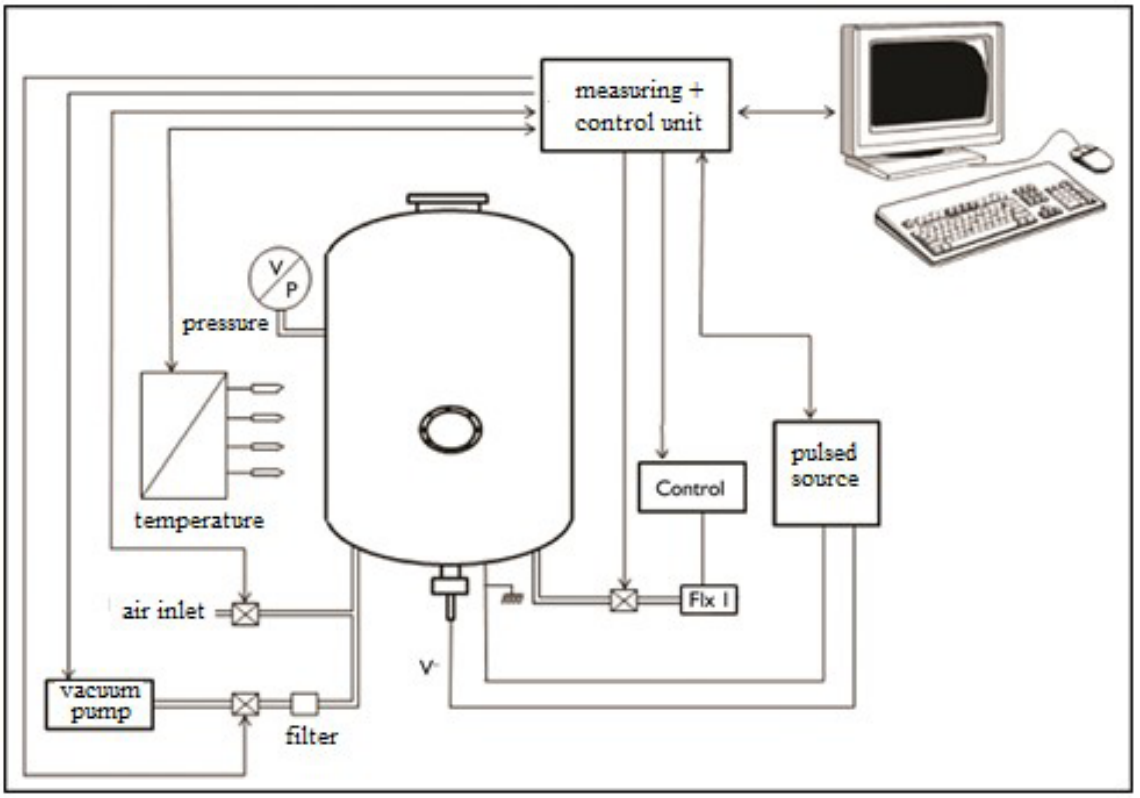

Figure 1. Schematic representation of the pulsed DC plasma reactor used of the plasma reduction experiments.

The preparation consisted in polishing with alumina, 0.3 µm. The samples were not etching with reagent and the images were obtained with the aid of a light microscope NEDA Metallux model brand and scanning electron microscope (SEM) Zeiss model EVO MA10 Collection was performed using voltage of 25 kV, in secondary electron detection mode on the SE1 detector.

3. Results and Discussion

Figure 2 shows the diffractogram Hematite powders before and after the plasma reduction experiments at 320 °C. Figure 2b shows the Hematite reducing (Fe_2O_3) at temperature of 320 °C after 30 min. In this condition is possible to see that the magnetite phase (Fe_2O_3) appear. After 60 min, Figure 2c, shows the presence of metallic iron (Fe-α) and magnetite (Fe_2O_3), no detecting Hematite (Fe_2O_3). Increasing time for 120 minutes, Figure 2e, where the diffractogram is not differ from that submitted to reduction for 90 min (Figure 2d).

Figure 3 shows the diffractogram Hematite powders before and after the plasma reduction experiments at temperatures at 340 °C. Figure 3b shows that the temperature at 340 °C, during 30 min., the Fe (Fe-α) is associated with the Hematite (Fe_2O_3), evidencing that the increasing temperature at 320 °C to 340 °C favoring the appearing of Fe-α in a lower time. Until 60 min, the Fe_2O_3 is not present, evidencing only peaks related to magnetite (Fe_3O_4) and metallic iron (Fe-α).

Evolution of the phases present in Hematite powders before and after reduction in the temperature of plasma 340 °C for times of 30 min (b), 60 min (c), 90 min (d) and (e) 120 min.

Figure 4 shows the diffractogram hematite powders before and after the plasma reduction experiments at temperatures at 360 °C. Increasing the temperature to 360 °C (Figure 4), in the first 30 minutes of reduction, did not detect of Hematite traces (Fe_2O_3), appearing only peaks of magnetite (Fe_3O_4) and of metallic iron (Fe-α), Figure 4b. With the increase of reduction process time, Figures 4b, 4c, 4d and 4e, it's possible to observe that there is an increase in the relative intensities of the peaks of Fe to the detriment of Fe_3O_4.

Figure 5 shows the diffractogram Hematite powders before and after the plasma reduction experiments at 380 °C. At this temperature, after 30 min of reduction (Figure 5b),

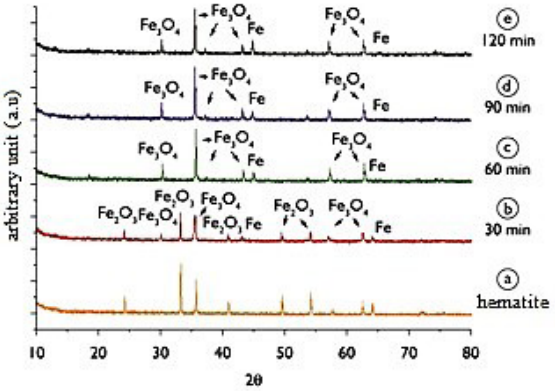

Figure 3. Phases generated in the process Hematite reduction by hydrogen at 340 °C in times of 30 min. (b), 60 min. (c), 90 min. (d) and (e) 120 min.

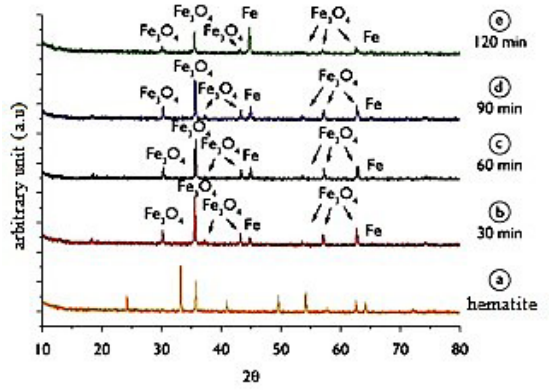

Figure 4. Phases generated in the process Hematite reduction by hydrogen at 360 °C in times of 30 min. (b), 60 min. (c), 90 min. (d) and (e) 120 min.

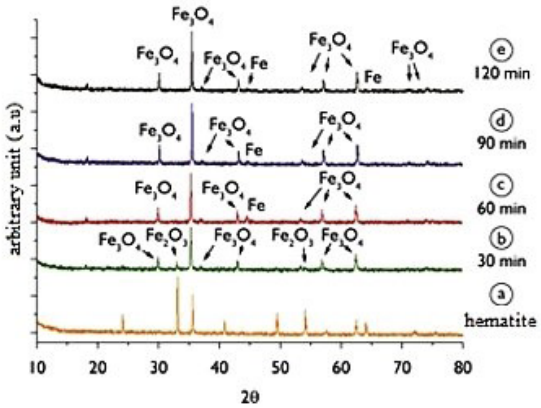

Figure 2. Phases generated in the process Hematite reduction by hydrogen at 320 °C in times of 30 min. (b), 60 min. (c), 90 min. (d) and (e) 120 min.

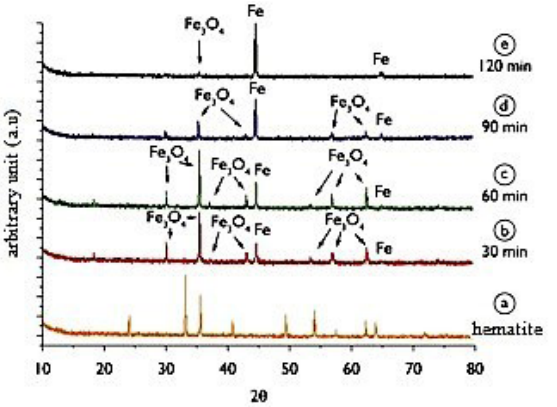

Figure 5. Phases generated in the process Hematite reduction by hydrogen at 380 °C in times of 30 min. (b), 60 min. (c), 90 min. (d) and (e) 120 min.

the Fe-α is associated with magnetite (Fe_3O_4), not detecting the presence of Hematite (Fe_2O_3). Comparing Figure 5b and Figure 2e it is possible observe that for the reduced powder at 380 °C for 30 min., the relative peak to Fe-α (111) presents intensity higher than the same peak relative to powder reduced at 320 °C for 120 min, evidencing that the amount of phase Fe-α after reduction at 380 °C for 30 min is higher than that obtained after reduction at 320 °C for 120 minutes. Increasing reduction process time to 120 minutes, Figure 5e, it's possible to observe only the presence of metallic iron (Fe-α) and some traces of magnetite (Fe_3O_4).

Therefore, the results of XRD indicate that the formation of the phase Fe-α is favored by increasing both the time and the temperature. The gaseous reduction of hematite occurred in two steps: $Fe_2O_{3(s)} \rightarrow Fe_3O_4$ (s) $\rightarrow Fe_{(\alpha)}$, as observed in Figure 5.

3.1. Kinetic model

Figure 6 shows the results of reacted fraction (α) versus time for each temperature of hematite reduction after the experiments of plasma reduction. According the results of x-ray diffraction, it is possible conclude that both the temperature and the time of reduction process are variables that have strong influence on reduction of Hematite. The different conditions of time and temperature possibility obtaining values of α that ranged from 0.08 (320 °C, 30 min) to 0.93 (380 °C, 120 minutes).

3.1.1. Reaction rate constants and activation energy

Rajput et al.[12] presented that the hematite reduction by hydrogen at lower temperatures 573K is only possible with the presence of cold plasma. The use of the plasma reduces the activation energy for reduction of Hematite from 46.78 kJmol to 5.07 kJmol. Therefore, the presence of plasma possibility the reduction process at lower temperatures when compared with molecular hydrogen, H_2 (g). Although it is known that in the cold hydrogen plasma consists of various species such as H_2 molecules, excited hydrogen molecules (H_2*), atomic hydrogen (H), ionic hydrogen (H^+), and free electrons., Rajput et al.[12] attributed the efficiency of the plasma reduction process relative to a gas reduction process to the vibrationally excited hydrogen molecules present in the plasma. Rajput et al.[12] does not explain clearly, as were obtained portions of reduction attributed to each of the possible species such as H, H^+ and $H_{2\ (excited)}$. In the case of reduction by atomic hydrogen (H), ionic hydrogen (H^+), global reactions are as follows (Reactions 2 and 3):

$$Fe_2O_{3(s)} + 6H^+ + 6e^- \Rightarrow 2Fe_{(s)} + 3H_2O_{(g)} \quad (2)$$

$$\Delta G0 = -8847 - 78{,}8 \times 10{-}3\ T\ [kJ/mol]$$

$$Fe_2O_{3(s)} + 6H \Rightarrow 2Fe_{(s)} + 3H_2O_{(g)} \quad (3)$$

$$\Delta G0 = -1072 - 88{,}4 \times 10{-}3\ T\ [kJ/mol]$$

In the step of reducing hematite by hydrogen at temperatures below 417°C, it was verified that the kinetic equation that best fits the experimental data is the Johnson-Mehl-Avrami-Erofe'ev-Kolmogorov[20-22] (JMAEK) equation, tridimensional model, phase boundary reaction (contracting sphere) (Equation 4):

$$1-(1-\alpha)^{1/3} = k.t \quad (4)$$

where: α is the fraction of reduction and k is the temperature-dependent reaction rate constant and t is the time of reduction.

The hematite reduction particles by hydrogen plasma, it possible consider, that physically has a spherical solid is circled by a fluid. Using the unreacted nuclei model, widely used for molecular hydrogen reduction processes, Figure 7,

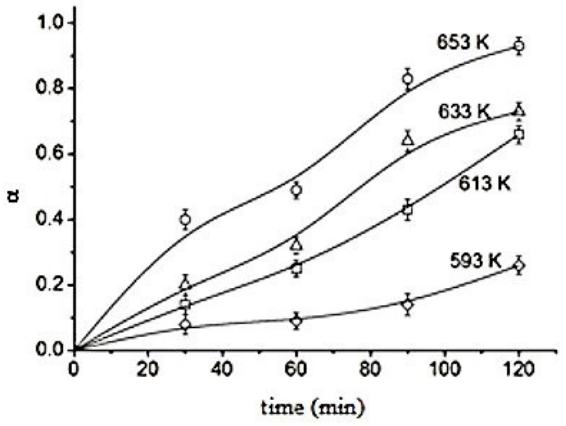

Figure 6. Reduction in Plasma, reacted fraction (α) versus time for each temperature.

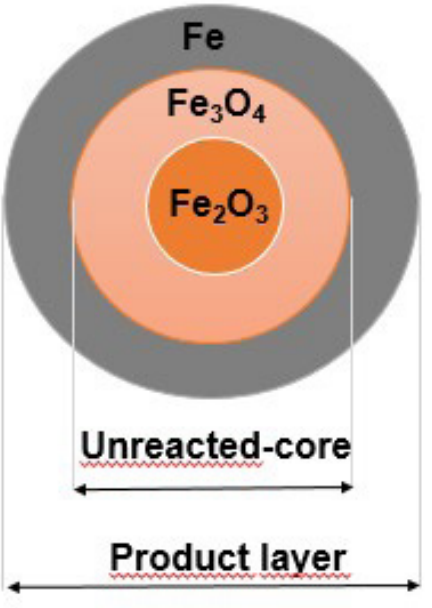

Figure 7. Schematic of a partially reduced spherical Hematite particle in lower temperatures at 580 °C.

adapted to the reduction process by cold plasma. In this case we have the central part surrounded by a layer of metallic iron product and finally reducing species as: H, H^+ and others, according with the reports of Rajput et al.[12]. In this work, the plasma reduction experiments were performed below 570° C, and it was not verified the formation of wustite (FeO). For the reduction of hematite particles with gaseous hydrogen, has been that the steps involved so that the process of reduction to occur are: I) diffusion of reagents; II) phase boundary reaction; III) nucleation and growth of a new phase; Each of these step's work with a sort of "resistance" that added will determine the kinetics of the process.

Figure 8 present evaluation of activation energy (E_a). Turkdogan and Vinters[23] and Pineau et al.[24] studied the influence of particle size and temperature on the reduction process of hematite by hydrogen. These authors demonstrated that the reduction process at low temperatures (less than 693 °C) and hematite fine ore with a particle size less than 0.1 mm is controlled by a chemical reaction in the solid-gas interface. The same study showed that the activation energy for reduction of Hematite was E_a = 87.5 kJmol for temperatures less than 690 K. According this study, Figure 8, it was obtained the value of E_a = 98.4 kJmol for global reaction, the same order of magnitude obtained by Pineau et al.[24]. This difference may be associated with the plasma power used and type of equipment and particle size[23-30].

3.2. Morphological aspects after hematite reduction

Figure 9 shows some particle agglomerates typically found after Hematite reduction by hydrogen plasma. At 380 °C, increasing the reduction time of 30 to 120 minutes, may observe that, practically all the darker portions of the agglomerates, turned into lighter portions. The lighter parts probably correspond to metallic iron while the dark match magnetite, as show the diffractograms presented in Figure 5b and Figure 5e. In this case, the value of the reacted fraction "α" increase for 0.40 (30 minutes) to 0.93 (120 minutes). These results obtained, through metallographic analysis, corroborate with the results obtained by mass balance and x-ray diffraction.

Figure 10a-c presents agglomerates of iron oxide after hematite reduction experiments at 380 °C for 120 minutes and the EDS results microanalysis performed in regions 1 (periphery) and 2 (center), respectively. The results of chemical microanalysis by energy dispersive spectroscopy (EDS) of region 1 (peripheral region) presents around 95% of iron and 5% oxygen, indicating that the region 1 is practically composed of Fe-α. The results of chemical microanalysis by energy dispersive spectroscopy (EDS) of region 2 (central region) indicating that the region 2 is composed of the Fe-α and Fe_3O_4 phases.

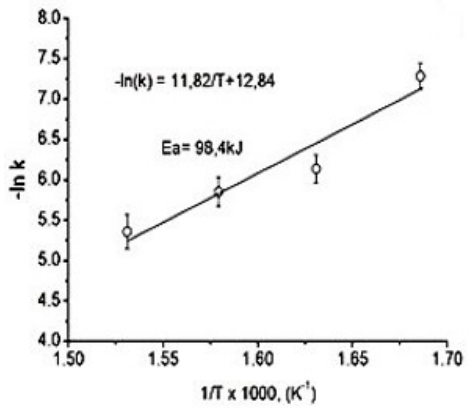

Figure 8. Arrhenius plot - evaluation of activation energy of hematite reduction process by hydrogen.

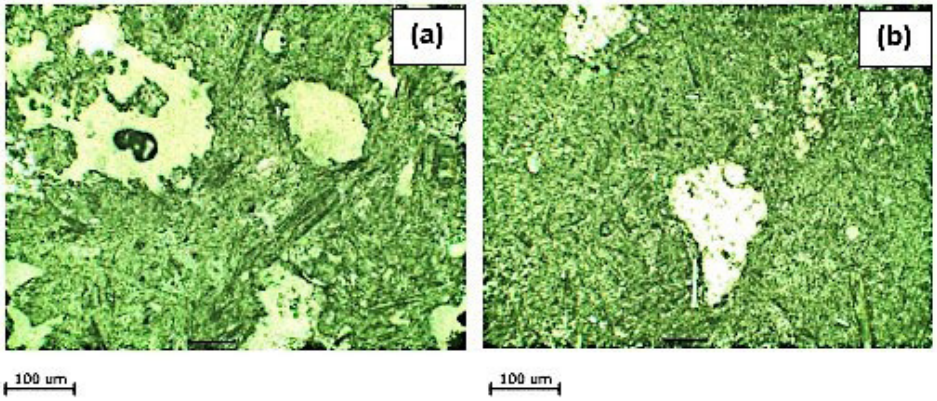

Figure 9. Cross-section of clusters of Hematite particles after plasma reduction in the temperature of 380 °C by: (a) 30 min (a) and (b) 120 min.

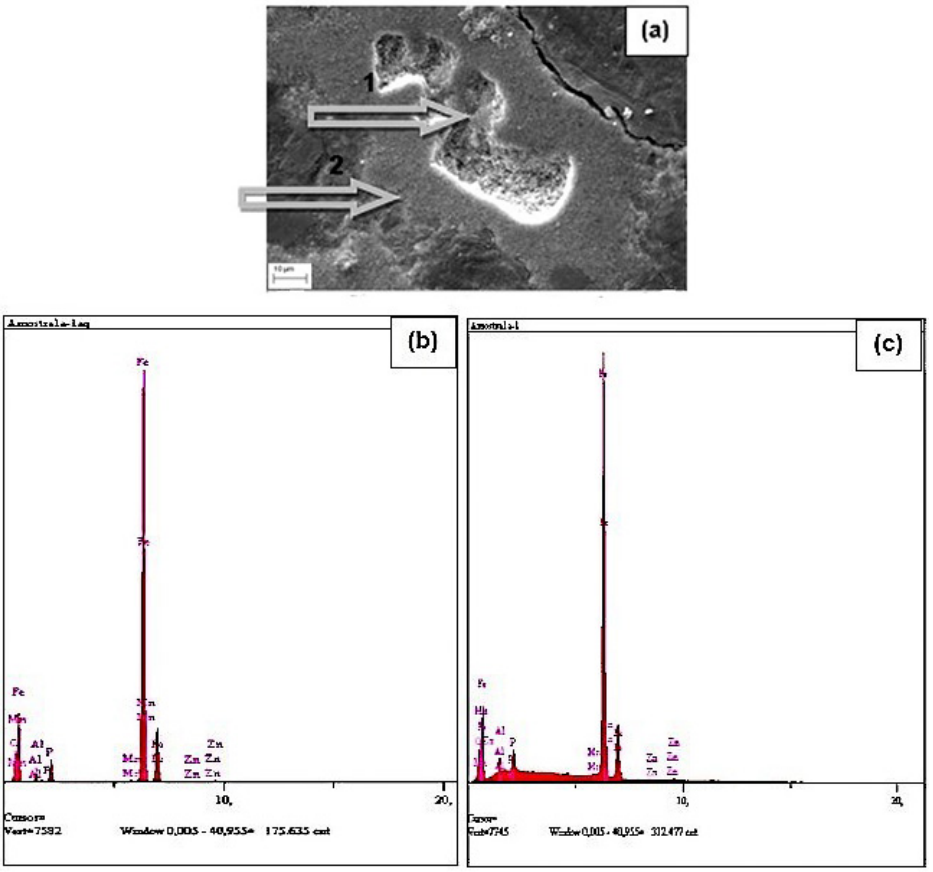

Figure 10. (a) Iron oxide cluster particles after plasma reduction at temperature of 380 °C for 120 min, (b) EDS microanalysis of region 1 (peripheral region), (c) microanalysis of region 2 (center region).

4. Conclusions

Through experimental data, this study concluded, conformed what was demonstrated in previous works, the reduction process at temperatures of 320 and 380 °C occurred in two steps: $Fe_2O_3 \rightarrow Fe_3O_4 \rightarrow Fe$. The high kinetics of oxide reduction at low temperature is associated with the action of reducing species derived from molecular hydrogen present in the plasma and the generation of vacancies during ion bombardment. At temperatures between 320 and 380 °C, the reduction mechanism of iron oxide particles is predominantly controlled by topochemical reactions. The range of 320 to 380 °C, the activation energy for the reduction of iron oxide, purity of 99.0% of Fe_2O_3, granulometry <5 μm, using cold hydrogen plasma as a reducing agent, was 97, 3 kJ/mol. X-ray diffraction analysis of partially agglomerated particles reduced under plasma revealed that on the periphery of the particle there are high concentrations of metallic iron, while in the interior region, there are high concentrations of oxygen, suggesting that the reduction process takes place from the surface to the nucleus.

5. Acknowledgments

We are grateful FAPES-Fundação de Amparo a Pesquisa-ES-Brasil, CNPq-Conselho Nacional de Desenvolvimento Científico e Tecnológico for the financial support. Capes-Coordenação de Aperfeiçoamento de Pessoal de Nível Superior, FINEP-Financiadora de Estudos e Projetos and IFES-Instituto Federal de Educação do Espirito Santo for their collaboration.The authors thank the direct financial support given by FINEP, CNPq through 2011-2012 Universal Edict and FAPES by granting master's scholarship.

6. References

1. Norgate TE, Jahanshahi S, Rankin WJ. Assessing the environmental impact of metal production processes. J Clean Prod. 2006;15(8):838-48.
2. Tien RH, Turkdogan ET. Gaseous reduction of iron oxides: part IV. Mathematical analysis of partial internal reduction-diffusion control. Metall Trans. 1972;3(8):2039-48. http://doi.org/10.1007/BF02643212.
3. Sastri MVC, Viswanath RP, Viswanathan B. Studies on the reduction of iron oxide with hydrogen. Int J Hydrogen Energy. 1982;7(12):951-5. http://doi.org/10.1016/0360-3199(82)90163-X.
4. Chen GZ, Fray DJ, Farthing TW. Direct electrochemical reduction of titanium dioxide to titanium in molten calcium chloride. Nature. 2000;407(6802):361-4. http://doi.org/10.1038/35030069.
5. Sabat KC, Rajput P, Paramguru RK, Bhoi B, Mishra BK. Reduction of oxide minerals by hydrogen plasma: an overview. Plasma Chem Plasma Process. 2014;34(1):1-23. http://doi.org/10.1007/s11090-013-9484-2.

6. Suryanarayana C. Mechanical alloying and milling. Prog Mater Sci. 2001;46(1-2):1-184. http://doi.org/10.1016/S0079-6425(99)00010-9.
7. Halmann M, Frei A, Steinfeld A. Vacuum carbothermic reduction of Al_2O_3, BeO, MgO-CaO, TiO_2, ZrO_2, $HfO_2 + ZrO_2$, SiO_2, $SiO_2 + Fe_2O_3$, and GeO_2 to the metals: a thermodynamic study. Miner Process Extr Metall Rev. 2011;32(4):247-66. http://doi.org/10.1080/08827508.2010.530723.
8. Peña MA, Gómez JP, Fierro JLG. New catalytic routes for syngas and hydrogen production. Appl Catal A Gen. 1996;144(1-2):7-57. http://doi.org/10.1016/0926-860X(96)00108-1.
9. Silva GG. Estudo da redução do trióxido de tungstênio ativado por plasma de hidrogênio [tese]. Natal: Universidade Federal do Rio Grande do Norte; 2003.
10. Zhang Y, Ding W, Lu X, Guo S, Xu K. Reduction of metal oxide in nonequilibrium hydrogen plasma. Zhongguo Youse Jinshu Xuebao. 2004;14(2):317-21.
11. Zhang Y, Ding W, Lu X, Guo S, Xu K. Reduction of TiO_2 with hydrogen cold plasma in DC pulsed glow discharge. Trans Nonferrous Met Soc China. 2005;15(3):594-9.
12. Rajput P, Bhoi B, Sahoo S, Paramguru RK, Mishra BK. Preliminary investigation into direct reducion of iron in low temperature hydrogen plasma. Ironmak Steelmak. 2013;40(1):61-8. http://doi.org/10.1179/1743281212Y.0000000023.
13. Nakayama MCY. Estudo da cinética de redução do óxido de cobalto (CO_3O_4) por plasma de hidrogênio em baixas temperaturas [dissertação]. Vitória: Instituto Federal do Espírito Santo; 2013.
14. Ramos SV, Franco AR Jr, Nascimento RC, Vieira EA. Influência da temperatura na redução de óxido de cobre sob plasma frio de hidrogênio. In: 68º Congresso Anual da ABM; 2013 Jul 30-Ago 2; Belo Horizonte, Brasil. Anais. São Paulo: Associação Brasileira de Metalurgia, Materiais e Mineração; 2013. p. 2094-103.
15. Santos BB, Franco AR Jr, Vieira EA, Nascimento RC. Redução do óxido de estanho (SnO2) por plasma de hidrogênio em baixas temperaturas. In: 68º Congresso Anual da ABM; 2013 Jul 30-Ago 2; Belo Horizonte, Brasil. Anais. São Paulo: Associação Brasileira de Metalurgia, Materiais e Mineração; 2013. p. 2380-8.
16. Robino CV. Representation of mixed reactive gases on free energy (Ellingham-Richardson) diagrams. Metall Mater Trans, B, Process Metall Mater Proc Sci. 1996;27(1):65-9. http://doi.org/10.1007/BF02915078.
17. Bullard DE, Lynch DC. Reduction of titanium dioxide in a nonequilibrium hydrogen plasma. Metall Mater Trans, B, Process Metall Mater Proc Sci. 1997;28(6):1069-80. http://doi.org/10.1007/s11663-997-0061-z.
18. Kim JY, Rodriguez JA, Hanson JC, Frenkel AI, Lee PL. Reduction of CuO and Cu_2O with H_2:H embedding and kinetic effects in the formation of suboxides. J Am Chem Soc. 2003;125(35):10684-92. http://doi.org/10.1021/ja0301673.
19. Chapman BN. Glow discharge processes. New York: John Wiley & Sons; 1980.
20. Sharda T, Misra DS, Avasthi DK, Mehta GK. Dissociation kinetics of molecular hydrogen in a microwave plasma and its influence on the hydrogen content in diamond films. Solid State Commun. 1996;98(10):879-83. http://doi.org/10.1016/0038-1098(96)00040-3.
21. Viswanath RP, Viswanathan B, Sastri MVC. Kinetics and mechanism of reduction of ferric oxide by hydrogen. Transactions of the Japan Institute of Metals. 1977;18(3):149-54. http://doi.org/10.2320/matertrans1960.18.149.
22. Wimmers OJ, Arnoldy P, Moulijn JA. Determination of the reduction mechanism by temperature-programmed reduction: application to small iron oxide (Fe_2O_3) particles. J Phys Chem. 1986;90(7):1331-7. http://doi.org/10.1021/j100398a025.
23. Turkdogan ET, Vinters JV. Gaseous reduction of iron oxides: part I. Reduction of Hematite in Hydrogen. Metall Trans. 1971;2(11):3175-88. http://doi.org/10.1007/BF02814970.
24. Pineau A, Kanari N, Gaballah I. Kinetics of reduction of iron oxides by H_2: part I: low temperature reduction of magnetite. Thermochim Acta. 2007;456(2):75-88. http://doi.org/10.1016/j.tca.2007.01.014.
25. Kuila SK, Chatterjee R, Ghosh D. Kinetics of hydrogen reduction of magnetite ore fines. Int J Hydrogen Energy. 2016;41(22):9256-66. http://doi.org/10.1016/j.ijhydene.2016.04.075.
26. Guo D, Hu M, Pu C, Xiao B, Hu Z, Liu S, et al. Kinetics and mechanisms of direct reduction of iron ore-biomass composite pellets with hydrogen gas. Int J Hydrogen Energy. 2015;40(14):4733-40. http://doi.org/10.1016/j.ijhydene.2015.02.065.
27. Barde AA, Klausner JF, Mei R. Solid state reaction kinetics of iron oxide reduction using hydrogen as a reducing agent. Int J Hydrogen Energy. 2016;41(24):10103. http://doi.org/10.1016/j.ijhydene.2015.12.129.
28. Gonoring TB, Franco AR Jr, Vieira EA, Nascimento RC. Kinetic analysis of the reduction of hematite fines by cold hydrogen plasma. J Mater Res Technol. 2022;20:2173-87. http://doi.org/10.1016/j.jmrt.2022.07.174.
29. Chen Z, Dang J, Hu X, Yan H. Reduction kinetics of hematite powder in hydrogen atmosphere at moderate temperatures. Metals. 2018;8(10):751. http://doi.org/10.3390/met8100751.
30. Zarl MA, Ernst D, Cejka J, Schenk J. A new methodologicalapproach to the characterization of optimal charging rates at thehydrogen plasma smelting reduction process part 1. Materials. 2022;15(14):4767. http://doi.org/10.3390/ma15144767.